



Ice-nucleating particles active below $-24\text{ }^{\circ}\text{C}$ in a Finnish boreal forest and their relationship to bioaerosols

Franziska Vogel^{1,a}, Michael P. Adams², Larissa Lacher¹, Polly B. Foster², Grace C.E. Porter^{2,8}, Barbara Bertozzi^{1,b}, Kristina Höhler¹, Julia Schneider¹, Tobias Schorr¹, Nsikanabasi S. Umo¹, Jens Nadolny¹, Zoé Brasseur³, Paavo Heikkilä⁴, Erik S. Thomson⁵, Nicole Büttner¹, Martin I. Daily², Romy Fösig¹, Alexander D. Harrison², Jorma Keskinen⁴, Ulrike Proske^{2,6,c}, Jonathan Duplissy^{3,7}, Markku Kulmala³, Tuukka Petäjä³, Ottmar Möhler¹, and Benjamin J. Murray²

¹Institute of Meteorology and Climate Research, Karlsruhe Institute of Technology, Karlsruhe, Germany

²Institute of Climate and Atmospheric Science, School of Earth and Environment, University of Leeds, Leeds, United Kingdom

³Institute for Atmospheric and Earth System Research/Physics, Faculty of Science, University of Helsinki, Helsinki, Finland

⁴Aerosol Physics Laboratory, Physics Unit, Faculty of Engineering and Natural Sciences, Tampere University, Tampere, Finland

⁵Department of Chemistry and Molecular Biology, Atmospheric Science, University of Gothenburg, Gothenburg, Sweden

⁶Institute for Atmospheric and Environmental Sciences, Goethe University Frankfurt, Frankfurt am Main, Germany

⁷Helsinki Institute of Physics, University of Helsinki, Helsinki, Finland

⁸School of Physics and Astronomy, University of Leeds, Leeds, UK

^aNow at: Institute of Atmospheric Sciences and Climate (ISAC), National Research Council (CNR), Bologna, Italy

^bNow at: Laboratory of Atmospheric Chemistry, Paul Scherrer Institute, Villigen, Switzerland

^cNow at: Hydrology and Quantitative Water Management, Wageningen University, Wageningen, Netherlands

Correspondence: Benjamin J. Murray (b.j.murray@leeds.ac.uk), Franziska Vogel (f.vogel@isac.cnr.it)

Abstract.

Cloud properties are strongly influenced by ice formation, hence we need to understand the sources of ice-nucleating particles (INPs) around the globe. Boreal forests are known as sources of bioaerosol and recent work indicates that these dominate the INP spectra above $-24\text{ }^{\circ}\text{C}$. To quantify the INP population at temperatures below $-24\text{ }^{\circ}\text{C}$, we deployed a portable cloud expansion chamber (PINE) in a Finnish boreal forest from March 13, 2018 to May 11, 2018. Using the 6 min time resolution PINE data, we present several lines of evidence that INPs below $-24\text{ }^{\circ}\text{C}$ in this location are also from biological sources: an INP parameterization developed for a pine forest site in Colorado, where many INPs were shown to be biological, produced a good fit to our measurements; a moderate correlation of INP with aerosol concentration larger than $0.5\text{ }\mu\text{m}$ and the fluorescent bioaerosol concentration; a negative correlation with relative humidity that may relate to enhanced release of bioaerosol at low humidity from local sources such as the prolific lichen population in boreal forests. The absence of correlation with ultra-fine particles (3.5 to 50 nm) indicates that new particle formation events are not sources of INP. This study should motivate further work to establish if the commonality in bioaerosol ice nucleating properties between spring in Finland and summer in Colorado is more generally applicable to different coniferous forest locations and times, and also to determine to what extent these bioaerosols are transported to locations where they may affect clouds.



15 1 Introduction

The cloud phase (liquid, ice or mixed-phase) is a crucial property affecting the amount of incoming solar radiation that reaches the Earth's surface (Boucher et al., 2013; Matus and L'Ecuyer, 2017). Thus, clouds have an important role in the radiative budget of the Earth, and responses of clouds to a changing climate feedback are highly uncertain (Ceppi et al., 2017; Storelvmo, 2017; Murray et al., 2021). Cloud phase is strongly influenced by the presence of aerosol particles, specifically if these aerosol particles act as ice-nucleating particles (INPs) (Hoose and Möhler, 2012; Murray et al., 2012; Kanji et al., 2017).

INPs initiate heterogeneous ice nucleation in supercooled liquid cloud droplets, that could otherwise freeze homogeneously at a temperature of approximately $-36\text{ }^{\circ}\text{C}$ (Pruppacher and Klett, 2010; Herbert et al., 2015) or trigger ice formation from the vapor phase via deposition nucleation (Vali et al., 2015). Heterogeneous ice nucleation is of high relevance in the atmosphere. For example, modelling studies have shown that the reflectivity of cold boundary layer marine clouds is strongly dependent on the INP concentration, with more INP leading to a dramatically reduced cloud albedo (Vergara-Temprado et al., 2018). Clouds resulting from deep convection are also strongly sensitive to INPs. In this case, the INP spectrum is important, where INP at around $-5\text{ }^{\circ}\text{C}$ trigger the Hallett-Mossop process, whereas INP active below $\approx -25\text{ }^{\circ}\text{C}$ are key in defining how much liquid water reaches homogeneous freezing ($\approx -36\text{ }^{\circ}\text{C}$) and therefore the microphysical properties of anvil cirrus (Takeishi and Storelvmo, 2018; Hawker et al., 2021a, b). Measurements using ground- and space-based remote sensing tools also indicate a relationship between cloud phase and aerosol (Choi et al., 2010; Kanitz et al., 2011; Villanueva et al., 2021) and there are many cases where cloud glaciation occurs at much higher temperatures than can be accounted for by homogeneous freezing or overseeding (Radenz et al., 2021).

Given the dependence of clouds on primary ice formation and the variability of INP concentrations around the globe, cloud phase in global climate models should be tied to the INP population in the atmosphere (Murray et al., 2021). However, our ability to do this is limited by our understanding of the sources, transport, interaction with clouds and sinks of the various aerosol species that have the capacity to nucleate ice (Hoose et al., 2010; Vergara-Temprado et al., 2017; Schill et al., 2020).

To date there is no robust predictor to provide information on how ice active an aerosol particle is, so we rely on measurements that quantify which and how many atmospheric aerosol particles serve as an INP. The most discussed INP types in literature are mineral dust from low latitude deserts (Chou et al., 2011; Niemand et al., 2012; Atkinson et al., 2013) and high latitude dust (Tobo et al., 2019; Sanchez-Marroquin et al., 2020; Barr et al., 2023), marine organics and sea spray aerosol (Wilson et al., 2015; DeMott et al., 2016; Irish et al., 2017; Wilbourn et al., 2020), volcanic ash (Mangan et al., 2017; Fahy et al., 2022) and some anthropogenic emissions such as combustion ashes (Umo et al., 2015; Grawe et al., 2016) or agricultural emissions (O'Sullivan et al., 2014; Steinke et al., 2016; Hiranuma et al., 2021). The general picture is that biological INP, including primary biological particles and biogenic aerosol, are thought to be important at temperatures above approx. $-20\text{ }^{\circ}\text{C}$, whereas mineral dust is thought to be important at lower temperatures (Tobo et al., 2013; Hill et al., 2016; O'Sullivan et al., 2018; Schneider et al., 2021; Maki et al., 2023). However, our understanding of the specific sources of these biological INPs is poor, hence field measurements in locations where there is a potential for biological INP to be released are needed in order to try to understand and ultimately represent these sources in models. In this study, we focus on conducting INP measurements

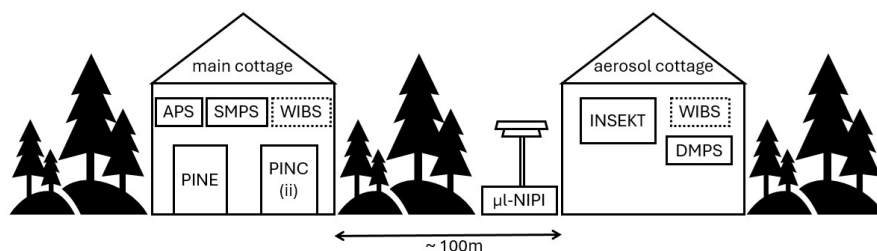


Figure 1. Overview of the instruments' measurement location at the SMEAR II station. Both, the main cottage and the aerosol cottage are located inside the forest. The dashed line around WIBS indicates that this instrument measured in both locations and was moved on April 3 from the main cottage to the aerosol cottage. All other instruments stayed at the same sampling location throughout the whole campaign.

in the boreal forest environment, making use of the well-established Station for Measuring Ecosystem-Atmosphere Relations (SMEAR) II located in Hyytiälä, Finland (Hari et al., 2013). Boreal forest is a known source of bio aerosols (Schumacher et al., 2013), but has not been extensively characterized in terms of its potential for producing INPs. SMEAR II is in operation since 1995, performing atmospheric and ecosystem measurements, and is well-known for frequent new particle formation events (Kulmala et al., 2001). This field site is set in a boreal forest made up of coniferous trees and is many kilometers from large urban centres or other anthropogenic aerosol sources. The HyICE-2018 campaign was launched in early 2018, a collaboration between 13 universities and institutions across 5 countries, with the aim of making ice-nucleating particle measurements in a boreal environment (Brasseur et al., 2022). The campaign was characterized by the transition period from winter to spring/summer during which the snow, with an initial depth of up to 60 cm, melted between end of March and mid April. In the present paper we report INP measurements between $-24\text{ }^{\circ}\text{C}$ and $-32\text{ }^{\circ}\text{C}$ under mixed-phase cloud conditions (i.e. at water saturation) using the Portable Ice Nucleation Experiment (PINE) chamber (Möhler et al., 2021). This was PINE's first field deployment. We have already shown that PINE compares well with other INP measurement techniques (Brasseur et al., 2022; Lacher et al., 2024) and the focus here is on using PINE for high temporal resolution INP measurements to determine the variability of the INP concentration below $-24\text{ }^{\circ}\text{C}$ and which aerosols types contribute to the INP spectra at these low temperatures in this boreal forest environment.

2 Methods

2.1 The PINE chamber

PINE is a mobile cloud expansion chamber, which was developed in 2017 and commercialized in 2019 (Möhler et al., 2021). PINE has been used for both field measurements of INPs (the first example of which is presented here) and in laboratory based studies (Ponsonby et al., 2024). In this study, the first prototype version, PINE-1A, was deployed, therefore the following description is specified for PINE-1A and its configuration during the HyICE-2018 campaign.



70 PINE-1A consists of five interconnected parts: the inlet system, the cloud expansion chamber, the cooling system, the particle
detection system and the control system. The inlet system contains a sampling tube connecting the ambient air inlet with two
parallel mounted nafion drying columns (Perma Pure, MD-700-24S-1). They are a crucial part of the inlet system, because
they remove humidity from the sampled air in order to prevent the inlet to the chamber to become blocked with ice. Behind
the dryers, a dew point sensor (dew point mirror MBW 973) monitors the humidity of the dried sampling air. For background
75 measurements sampling particle free air, an aerosol filter is manually installed between the ambient air inlet and the dryers.
The core of PINE is the cloud expansion chamber, which has a cylindrical shape with conical end caps and a volume of
approximately 7 L. Inside the chamber are three thermocouples, mounted with a 5 cm distance to the wall, measuring the gas
temperature at the top, in the middle and at the bottom of the chamber. On the same levels are another set of temperature sensors
glued to the wall to measure the temperature there. To cool the cloud expansion chamber to mixed-phase cloud temperatures, a
80 chiller (Lauda RP 855; Lauda-Königshofen, Germany) is used, where cooled ethanol flows through pipes wrapped around the
cloud expansion chamber. It can either hold the chamber at a constant temperature or perform a predefined temperature ramp
given the temperature to attain and the time to hold this temperature. Mounted on the bottom of the cloud expansion chamber
is an optical particle counter (OPC), which is, in this study, a combination of a welas® 2500 sensor and a Promo® 2000
control unit (Palas GmbH). The OPC detects larger aerosol particles, liquid cloud droplets and ice crystals as single particles,
85 based on the scattering signal. The welas® 2500 sensor only analyzes 10 % of the particles crossing the sensor, which leads
to a detection limit of approximately 5 L^{-1} . The control system, made of multiple flow controllers and a LabView software,
ensures a smooth operation of PINE bringing all the components together.

PINE operates in a continuous way, where sequences composed of the three modes named "flush mode", "expansion mode"
and "refill mode" are repeated constantly. During the flush mode the chamber is filled with air containing the aerosol under
90 investigation, and the pressure and the gas and wall temperature are held constant. When the aerosol population inside the
chamber is renewed, the expansion mode is started by closing the PINE inlet, while continuing to pump out air with a designated
flow rate. By pumping out air, the pressure inside the chamber decreases adiabatically and by that also the gas temperature.
Consequently, the saturation with respect to water and ice increase allowing liquid cloud droplets and ice crystals to form
once they exceed supersaturation. The expansion mode ends when the pressure reaches a pre-set value. The expansion mode is
95 followed by the refill mode, where the chamber is slowly filled up with particle free air to the initial pressure. At the end of the
refill mode, the chamber is reopened and the next flush mode begins. For each individual expansion mode an INP concentration
is calculated from the ratio of the number of ice crystal counts and the volume of analyzed air. The INP concentration is assigned
to the lowest temperature measured during the expansion mode with the gas temperature sensor at the bottom of the chamber.
The uncertainty for PINE is given as 20 % (Möhler et al., 2021) and is not displayed in the following figures to keep them
100 clear.

2.2 Installation and operation of PINE at SMEAR II

At the SMEAR II station, PINE was placed in the main cottage (Fig. 1) situated in the forest (Brasseur et al., 2022). The
other online INP counters, PINC (Portable Ice Nucleation Chamber, operated by EHT Zurich; Kanji et al. (2013)) and PINCii



(Portable Ice Nucleation Chamber ii, operated by University of Helsinki and University of Gothenburg; Castarède et al. (2023)),
105 were also installed in the main cottage. Results from these complementary instruments are presented in Paramonov et al. (2020)
and Brasseur et al. (2022). All instruments sampled from a heated total aerosol inlet positioned 6 m above ground level. Due
to the setup of the PINE chamber in the cottage, the inlet line contained some bends that resulted in the loss of larger aerosol
particles. An inlet characterization experiment using an OPC (MetOne, GT 526S) directly at the aerosol inlet and at the entrance
of PINE showed a 50 % cut-off for particles between 5 μm and 10 μm in diameter. In the size range between 3 μm and 5 μm ,
110 80 % of the particles were still able to enter the PINE chamber.

PINE was continuously operated from March 13, 2018 until May 11, 2018 in the temperature range of mixed-phase cloud
conditions between -24 °C and -32 °C. Most days PINE ran at a constant temperature between -28 °C and -30 °C and mea-
surements at the higher and lower ends of the broader temperature range were mainly reached while performing temperature
ramps. Temperature ramps were programmed to last approximately 3 h, in which the temperature was decreased every hour by
115 2 to 3 °C. The cooling times to attain the temperatures were in the range of a few minutes.

Each morning a background test was performed, to ensure that no frost artefacts are seen in the OPC signal, in order to
avoid miscounting ice crystals. For background tests, an aerosol particle filter is mounted between the ambient air inlet and
the dryers and the cloud expansion chamber is filled with particle free air. In this configuration, five expansions are conducted,
after which no ice crystals and almost no cloud droplets are counted by the OPC, showing that the chamber is fully clean.

120 Throughout the campaign, PINE was operated with the same settings for the flush, expansion and refill mode which were as
follows:

- Flush mode: flow of 3 Lmin^{-1} for a duration of 4 min
- Expansion mode: flow of 4 Lmin^{-1} until the pressure inside the chamber reaches 700 mbar
- Refill mode: flow of 3 Lmin^{-1} until the chamber is filled

125 Given these settings, the total duration of one sequence of flush mode, expansion mode and refill mode was approximately
6min.

2.3 Offline INP measurements

The online INP measurements of PINE are compared to two different offline INP methods, namely INSEKT (Ice Nucleation
Spectrometer of the Karlsruhe Institute of Technology) and μl -NIPI (μl Nucleation by Immersed Particles Instrument). Those
130 freezing assay techniques are described in detail in Schneider et al. (2021) and O'Sullivan et al. (2018), and only a short
explanation is given here. The specific methodology employed in HyICE-2018 is also described in Brasseur et al. (2022) and
the associated data are publically available in databases (<https://doi.org/10.5281/zenodo.10469663> and <https://doi.org/10.5445/IR/1000120666>). For both methods, aerosol particles are collected on 0.4 μm or 0.2 μm nuclepore filters using a defined flow
for a given time. The INSEKT filters used for comparison were sampled for 24 h in the aerosol cottage, about 100 m distant
135 from the main cottage, and μl -NIPI filters sampled for between 4 and 18 h using commercial samplers with PM10 inlet heads



(BGI PQ100, Mesa Laboratories Inc.). For the offline INP analysis, the aerosol loaded filters are washed into pure water to create a suspension containing the sampled aerosol. For INSEKT filter analysis, the original suspension is diluted 10 and 100 times, which allows the resulting INP-temperature spectrum to be extended towards temperatures as low as $-25\text{ }^{\circ}\text{C}$. The suspension is placed in $50\text{ }\mu\text{L}$ volumes in the wells of a PCR plate. As a freezing reference, a subset of wells are filled with
140 nanopure water. The PCR plates are placed in an aluminum block, which is cooled at a rate of 0.33 Kmin^{-1} to a temperature where all wells freeze. A camera records the freezing of the droplets and together with the temperature at which they froze an INP-temperature spectrum is obtained. For $\mu\text{l-NIPI}$ filter analysis, the suspension is pipetted to form an array of droplets of $1\text{ }\mu\text{L}$ volume on a hydrophobic glass slide. The glass slide is cooled with a rate of 1 Kmin^{-1} , until all droplets freeze. As with INSEKT, a camera records the freezing of the droplets.

145 **2.4 Additional aerosol and meteorological measurements**

SMEAR II is an aerosol and trace gas measurement site equipped with a large set of instrumentation measuring meteorological variables and aerosol properties (Hari et al., 2013; Junninen et al., 2009; Neeffjes et al., 2022). Extended descriptions of the instruments can be found in Schneider et al. (2021) and Brasseur et al. (2022), so here we briefly mention the instruments and measured variables utilized in this study.

150 Meteorological variables are measured at different heights above ground level on a 150 m meteorological mast. If possible, data closest to the inlet height of 6 m are utilized, however, some variables are only available at somewhat higher or lower levels. Table 1 summarizes the instrumentation and height at which the measurements are taken. Aerosol particle size distributions are measured with a DMPS, for diameters between 3 nm and 1000 nm, and with an APS the particles between $0.5\text{ }\mu\text{m}$ and $20\text{ }\mu\text{m}$ in diameter. The data are merged during analysis. For consistency, we work with the DMPS and APS data from Schneider et al.
155 (2021) and refer for further information to their work. A WIBS (Wideband integrated bioaerosol sensor) measures particle fluorescence with two excitation lasers, and emission is monitored in two detection bands. A fluorescence threshold is applied to differentiate highly fluorescent biological particles from weakly fluorescent particles like dust. The two lasers and the two detection bands allow detailed differentiation of particle types (Cornwell et al., 2023). During the campaign a WIBS-NEO (Droplet Measurement Technology) was operated. From March 11 until April 3, it was installed in the main cottage and
160 thereafter moved to the aerosol cottage. The cottages have inlets with a different size cut-off, specifically $5\text{ }\mu\text{m}$ in the main cottage and $10\text{ }\mu\text{m}$ in the aerosol cottage. The concentrations of the large particles measured with WIBS show no significant increase after the change of the location, so we use the data without applying a correction. More detailed information can be found in Schneider et al. (2021) and Brasseur et al. (2022).

3 Results

165 For two months, PINE measured the INP concentration continuously in a boreal forest for temperatures between $-24\text{ }^{\circ}\text{C}$ and $-32\text{ }^{\circ}\text{C}$, the lower temperature regime of mixed-phase cloud conditions.



Table 1. Overview of variables measured at SMEAR II and used here for data analysis. The information are divided into the measured variable, the instrument and the sampling height above ground level.

Variable	Instrument	Height above ground (m)
Wind speed	Thies 2D Ultrasonic anemometer	8.4
Wind direction	Thies 2D Ultrasonic anemometer	8.4
Temperature	Pt100 inside custom shield	4.2
Relative humidity	Rotronic MP102H RH sensor	16.8
Pressure	Druck DPI 260 barometer	ground
Precipitation	Vaisala FD12P weather sensor	18
Snowfall	Vaisala FD12P weather sensor	18
Snow depth	Jenoptik SHM30	ground
Aerosol size distr. 3 nm to 1000 nm	Differential mobility particle sizer (DMPS)	8
Aerosol size distr. 0.5 μm to 20 μm	Aerodynamic particle sizer (APS, TSI model 3320)	6
Fluorescent particles 0.5 μm to 30 μm	Wideband integrated bioaerosol sensor (WIBS)	6 (March 11 - April 3), 8 (April 3 - end)

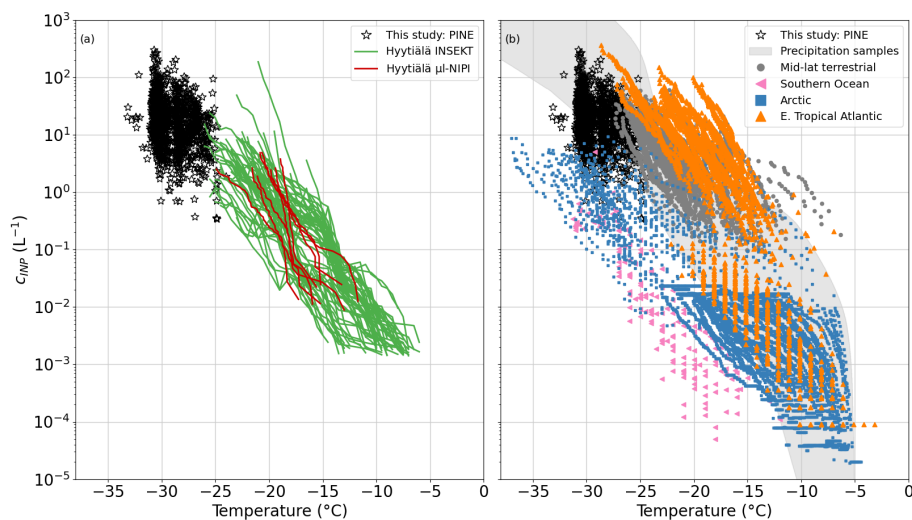


Figure 2. Comparison of INP concentrations (C_{INP}) measured with PINE (black stars), INSEKT (green lines) and μI -NIPI (red lines) during HyICE-2018 (a) and with INP measurements from a variety of locations around the world (b). The precipitation samples collected around the world (grey shading) originate from Petters and Wright (2015), the Arctic measurements (blue squares) are from Irish et al. (2019); Wex et al. (2019); Porter et al. (2022), those from the eastern tropical Atlantic (orange triangles) are from Price et al. (2018); Welti et al. (2018), the Mid-latitude terrestrial data (grey dots) is from O’Sullivan et al. (2018) and data from the southern ocean (pink triangles) from McCluskey et al. (2018).

Figure 2 provides an overview on how the 1 h time averaged PINE data from this monitoring (black stars) compares to the filter based measurements from the same campaign (Figure 2a) and measurements from various locations and source

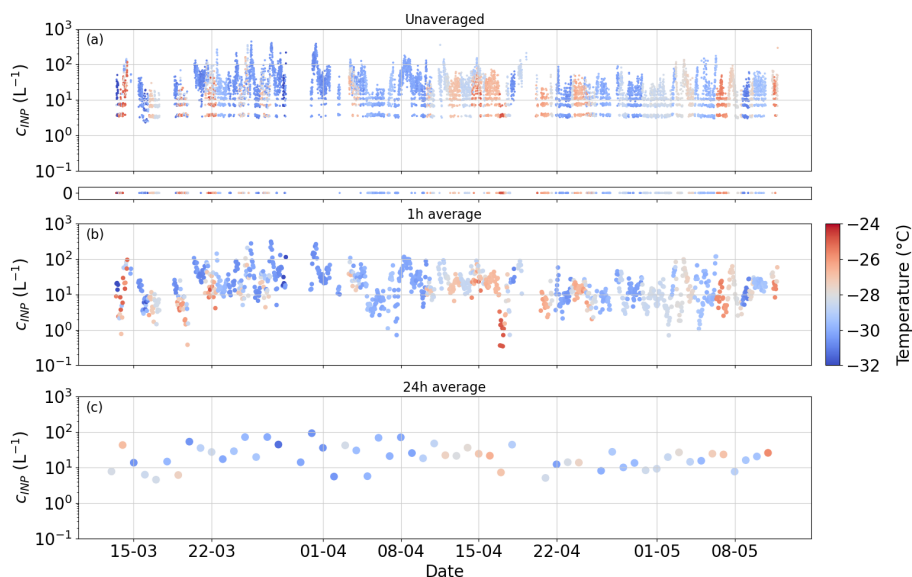


Figure 3. Time averaged PINE INP data over different periods. The measurements cover freezing temperatures between $-24^{\circ}C$ and $-32^{\circ}C$. (a) Shows the unaveraged PINE data, where each data point represents one expansion. The small panel below indicates the expansions in which no ice crystals were counted. (b) and (c) Contain the 1 h and 24 h time averages, respectively.

regions around the world (Figure 2b) acquired from filter samples, precipitation samples and continuous flow diffusion chamber
 170 measurements. For the given temperatures, the PINE INP measurements span two orders of magnitude from a minimum INP
 concentration of approximately $0.5 L^{-1}$ to $500 L^{-1}$. The PINE data mainly extend the INP spectra of INSEKT and μ l-NIPI
 towards lower temperatures. An overlap with INSEKT is only found at temperatures near $-25^{\circ}C$. Therefore, once combined,
 data from HyICE-2018 provide INP data from the Finnish boreal forest between $-6^{\circ}C$ and $-32^{\circ}C$ and thus cover almost the
 full mixed-phase cloud regime. In comparison to other locations, the PINE INP data compare best with INPs from mid-latitude
 175 terrestrial sources (grey dots). INP concentrations measured in the Arctic (blue squares) and southern ocean (pink triangles)
 are mainly lower, whereas INP measurements from the eastern tropical Atlantic (orange triangles) are mainly higher than what
 was measured in the boreal forest. So the INP concentration measured with PINE in Hyytiälä falls within the middle range of
 INP concentrations in comparison to a more global overview.

3.1 Time averaging PINE data

180 PINE measured INP concentrations with a time resolution of approximately 6 min, where from each expansion one data point
 was obtained (Figure 3a). The range of the unaveraged measured INP concentrations spreads over two orders of magnitude
 between $5 L^{-1}$ and approximately $500 L^{-1}$. These single expansion data show the same variation over the entire two months
 of the campaign, where very high and very low INP concentrations were measured within a few hours or days. Among all
 the performed expansions, about 10 % had 0 ice crystal counts and are therefore represented as an INP concentration of 0



185 L^{-1} . These 0 ice crystal runs occurred throughout the campaign and over almost the entire temperature range between $-24\text{ }^{\circ}\text{C}$
and $-32\text{ }^{\circ}\text{C}$ emphasizing the observed variation in the overall INP concentration. A quantisation of the data is visible, when
only 1, 2 or 3 ice crystals were counted during an expansion as stripes of data points at around 5, 8 and $10\text{ }L^{-1}$, respectively,
carrying a large counting error of \sqrt{n} . However, the daily background tests ensured that these low ice counts are associated
with INP, rather than frost artefacts from the chamber walls or other artefacts such as electrical noise. A detailed discussion of
190 the background measurements is given in Möhler et al. (2021). The non-averaged high time resolution data illustrate short-term
INP variability, but to improve counting statistics and compare with other data, some time averaging is needed. To improve the
counting statistics, we average over several expansions, thus also reducing the influence of instances where there are zero, or
very few ice crystals observed per expansion. With 1 h averages all zeros and quantized values are removed, while information
on the temporal evolution of the INP concentration is preserved (Figure 3b). In addition, 1 h averages lead to an order of
195 magnitude increase in the lowest detectable INP concentration. To compare the PINE measurements with offline INP methods
such as INSEKT and $\mu\text{l-NIPI}$, even longer time averaging, in this case 24 h, is needed (Figure 3c). By averaging such highly
time resolved data over one day, information about the short-term variation on a time scale of hours gets lost and only trends
on a longer time scale of days to weeks are pictured. This highlights that INP measurements with a high time resolution, as
done with PINE, over a long time period are important. Various time averages can be applied later, depending on the goal of
200 the analysis.

3.2 Comparison of temperature ramps of PINE with INSEKT and $\mu\text{l-NIPI}$

The consequences on the time averaging and the loss of short-term variations in the INP concentration can also be seen by
comparing PINE measurements to INSEKT and $\mu\text{l-NIPI}$ (Figure 4). An INSEKT filter was typically sampled for 24 h, while
 $\mu\text{l-NIPI}$ filters were sampled for 12 h (day/night) and PINE performed in the same time period six temperature ramps, where
205 one ramp lasts approximately 3.5 h. In this case three temperatures were set during the ramp resulting in data points scattered
by $\pm 2\text{ }^{\circ}\text{C}$ around the set temperature. To obtain a continuous spectrum, the data were binned in $1\text{ }^{\circ}\text{C}$ steps. The overlap in
temperature for INSEKT and PINE is only at $-24\text{ }^{\circ}\text{C}$ while PINE and $\mu\text{l-NIPI}$ do not overlap. However, PINE nicely extends the
INP-temperature spectrum towards lower temperatures. $\mu\text{l-NIPI}$ measurements overlap with INSEKT for the entire temperature
range. Comparing the day and night filters from $\mu\text{l-NIPI}$, one can see that the day filter is fully in the range of the INSEKT
210 filter for temperatures higher than $-18\text{ }^{\circ}\text{C}$, and the night filter shows up to one order of magnitude lower INP concentrations for
temperatures between $-18\text{ }^{\circ}\text{C}$ and $-20\text{ }^{\circ}\text{C}$. During the same sampling period, PINE performed six temperature ramps, which
show a variation of a factor of 5 over the captured temperature range. The PINE data at $-24\text{ }^{\circ}\text{C}$ is consistent with the INSEKT
data at that temperature. On average, the PINE measurements (black upside down triangles) align well with the INSEKT INP-
temperature spectrum and extend these measurements towards lower temperatures. This comparison is another illustration that
215 PINE is able to capture a short-term variability which would otherwise be missed with the filter-based measurements or when
averaging data.

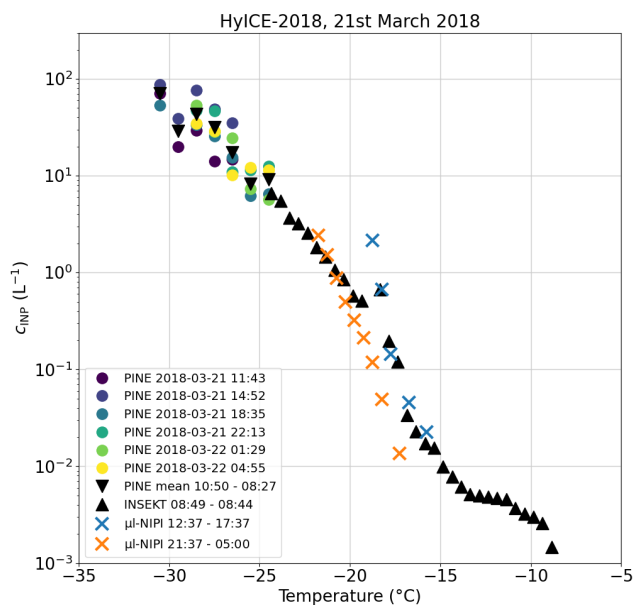


Figure 4. Comparison of the INP concentration of PINE temperature ramps with INSEKT and μ I-NIPI data in the sampling period of March 21. For the sampling period of the INSEKT filter (black triangles) the start and stop time are given, with the start day on March 21 and the stop day on March 22. The μ I-NIPI filters are divided into a day (orange cross) and a night (blue cross) filter. PINE measurements are split to the individual temperature ramps (colored dots) and an average of the full sampling period of PINE (black upside down triangles). The times of the individual PINE temperature ramps are the times when half the ramp is over.

3.3 Comparison of measured INP concentrations to those predicted with literature parameterizations

To represent primary ice formation in the atmosphere in models, a number of parameterizations have been developed and relate the INP concentration to various properties of the aerosol population or to meteorological variables. Here, we compare our PINE INP measurements with four parameterizations that we consider the most suitable for the measurement location. Those are from DeMott et al. (2010), based on measurements in various locations and different aerosol types, Tobo et al. (2013), who used data acquired in a conifer forest in summertime to present two different parameterizations, and Schneider et al. (2021) making use of measurements during the same campaign using INSEKT data. Hereafter, the four parameterizations are referred to as DeMott 2010, Tobo 2013 (1), Tobo 2013 (2) and Schneider 2021. DeMott 2010 and Tobo 2013 (1) base their INP concentration predictions on the concentration of aerosol particles larger than $0.5 \mu\text{m}$ in diameter, Tobo 2013 (2) uses the concentration of fluorescent particles with a diameter larger than $0.5 \mu\text{m}$ and Schneider 2021 found the ambient air temperature to be a predictive parameter. The valid temperature ranges for DeMott 2010 and Tobo 2013 (1) and (2) are given from $-15 \text{ }^\circ\text{C}$ to $-35 \text{ }^\circ\text{C}$ and $-5 \text{ }^\circ\text{C}$ to $-35 \text{ }^\circ\text{C}$, respectively, covering the full temperature range of the PINE measurements. Schneider 2021 is limited to temperatures between $-5 \text{ }^\circ\text{C}$ and $-25 \text{ }^\circ\text{C}$, which is mainly outside the range of the PINE measurements. However,

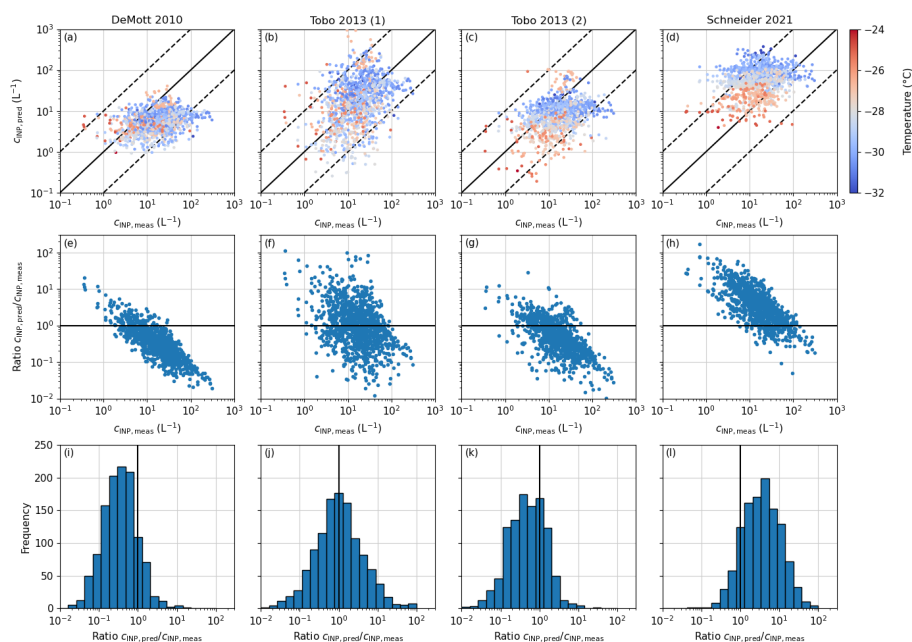


Figure 5. Predictions for PINE INP concentration using the parameterizations of DeMott 2010 (a), Tobo 2013 (1) and (2) (b) and (c) and Schneider 2021 (d). The solid line represents the 1:1 line and the dashed lines are a factor of 10 lower and higher than the 1:1 line. The plots in the second row ((e), (f), (g) and (h)) represent the evolution of the ratio of the predicted INP concentration ($c_{\text{INP,pred}}$) to the measured INP concentration ($c_{\text{INP,meas}}$) with an increasing measured INP concentration. The solid line is unity, where the prediction matches exactly the measured value. (i), (j), (k) and (l) are histogram representations of the ratio $c_{\text{INP,pred}} / c_{\text{INP,meas}}$, where the solid line is again unity.

230 since it is based on measurements in the same location and during the same time period, it is still valuable to apply this parameterization to our data.

Applying DeMott 2010, Tobo 2013 (1) and (2) and Schneider 2021 to our PINE data to test them for their predictive capability, 1 h time averaged data were used to align the INP data with the aerosol data from the SMEAR II APS. DeMott 2010 tends to underpredict the majority of the data by a factor of 5 to 10 (Figure 5a). In order to highlight the offset from the 1:1 line, the ratio of the predicted to the measured INP concentration ($c_{\text{INP,pred}} / c_{\text{INP,meas}}$) was calculated, where one is a perfect prediction, values larger than one indicate an overprediction of the parameterization and smaller values an underprediction. In the case of DeMott 2010, a clear trend from overprediction to underprediction is visible for increasing INP concentrations (Figure 5e). This corresponds to the temperature dependence of the parameterization being too shallow. The corresponding frequency histogram in Figure 5i peaks between 0.5 and 0.7 showing that the majority of the data points remains within a factor of 10. Moreover, DeMott 2010 gives a variation in the INP concentration of generally less than two orders of magnitude, whereas the measured INP concentrations vary by almost three orders of magnitude.

240 Comparing our PINE INP data with Tobo 2013 (1) predictions, the data are scattered around the 1:1 line with the majority of data within a factor of 10 (Figure 5b). For Tobo 2013 (1), the $c_{\text{INP,pred}}$ to $c_{\text{INP,meas}}$ ratio indicates a slight trend towards an



underprediction for higher INP concentrations (Figure 5f), but less pronounced than for DeMott 2010. The frequency histogram
245 in Figure 5j shows a symmetric distribution around unity, underlining that overall Tobo 2013 (1) predicts the INP concentration
well, which could be because it is based on measurements in a coniferous forest with similar biological INP sources to those
in the boreal forest in Finland.

When using the concentration of fluorescent particles as a predictive parameter in Tobo 2013 (2), the INP concentration tends
to be underpredicted by about a factor of 2 (Figure 5c). As for DeMott 2010, low INP concentrations were more overpredicted
250 than higher INP concentrations (Figure 5g). The histogram (Figure 5k) has a wide peak between 0.5 and 1. This means that the
measured INP concentration from the boreal forest in Finland cannot be predicted by biogenic particles (as measured by the
WIBS) only, but is rather a combination of biogenic particles and larger aerosol particles from different sources.

In contrast to DeMott 2010 and Tobo 2013 (2), Schneider 2021 overpredicts the INP measurements, with larger deviations
at lower temperatures (about one order of magnitude below -28°C ; Figure 5d). At temperatures that overlap with the INSEKT
255 data (-24 to -25°C) the agreement between the parameterization and PINE measurements is much better. Compared to DeMott
2010 and Tobo 2013, Schneider 2021 links INP concentration to the ambient air temperature to represent the seasonality
in the INP concentration. The ratio of predicted to measured INP concentration in Figure 5g shows a clear overprediction
for lower INP concentrations and an underprediction for the higher measured INP concentrations. Also the frequency plot
in Figure 5l shows a symmetric distribution with a peak between five and seven. The discrepancies applying the Schneider
260 2021 parameterization may originate from the valid temperature range, which is above -25°C . Furthermore, the INP data
measured with PINE have a less pronounced temperature dependence compared to those measured with INSEKT, which could
be due to a different portion of the aerosol particle population serving as INP in the respective temperature regimes. Moreover,
freezing assays like INSEKT measure only INPs from the immersion freezing mode, while PINE can also capture deposition
and condensation nucleation. At temperatures higher than -36°C , the temperature at which water freezes homogeneously,
265 the contribution of deposition/condensation nucleation is thought to be low (Westbrook and Illingworth, 2011), but may still
explain some of the discrepancies.

3.4 Correlation of INP concentration with aerosol and meteorological variables

Driving factors for changes in the INP concentration can vary, as is hinted at in the application of the different predictive
parameters used for the DeMott 2010, Tobo 2013 (1) and (2) and Schneider 2021 parameterizations. Only the Tobo 2013 (1)
270 parameterization predicted the measured INP concentration within one order of magnitude. To further investigate potential
connections between ice nucleation activity and meteorological variables and aerosol properties at temperatures lower than -25°C ,
correlation coefficients are calculated. The correlations are calculated using the Spearman correlation coefficient. Here, we
also present the p-value connected to each correlation coefficient, indicating whether a correlation is statistically significant
($p < 0.05$) or not ($p > 0.05$). Correlations for all meteorological variables listed in Table 1, as well as some aerosol properties and
275 'time over land' and the INP concentration are displayed in Figure 6. The time over land is a parameter determined from back-
trajectory analysis and corresponds to the time an air mass spends over the boreal forest environment before being measured
at the SMEAR II station. For the correlation analysis, only air masses from the corridor between north and west of Hyytiälä,

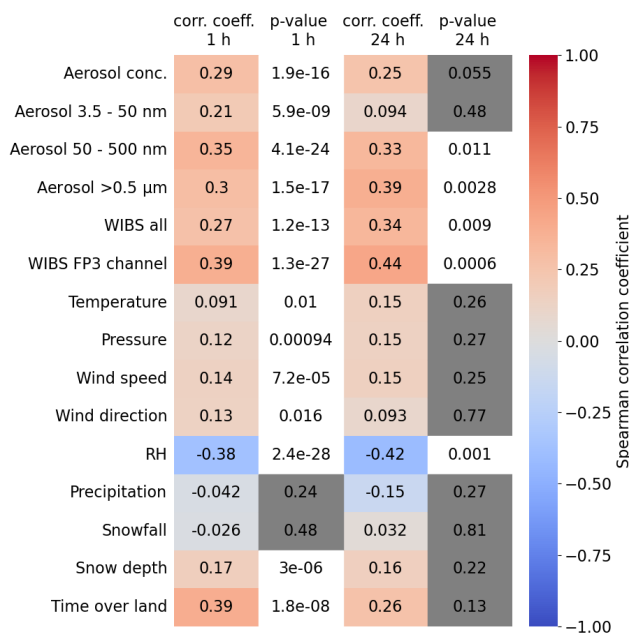


Figure 6. Spearman correlation coefficient calculated for full campaign period using 1 h and 24 h time averages of the PINE INP data. The temperature range of PINE measurements was limited to temperatures between -27 °C and -30 °C. Red colors represent a positive correlation, whereas blue colors indicate a negative correlation. The p-values marked with grey boxes indicate $p > 0.05$, i.e. the correlation is not considered to be statistically significant.

the so-called clean sector, are considered to eliminate potential continental aerosol sources. More information concerning this parameter and the way it is calculated can be found in Petäjä et al. (2022). To limit biases in the correlations due to the wide temperature range of the PINE measurements, only data points between -27 °C and -30 °C are considered, which includes the majority of all data and covers the entire time range. In Figure 6, we show the correlation coefficients for 1 h averaged data as well as the 24 h averaged data. The correlation coefficients are generally not significantly different between the two time averages, however, the p-value gives more statistical significance to the 1 h averages, so we focus the discussion on that data.

The highest positive correlations, albeit still weak, are found between INP concentration and the WIBS, FP3 channel, indicating tryptophan (0.39), which was also reported by Cornwell et al. (2023) and the time over land (0.39). The time over land considers air masses coming from the clean sector as defined in Petäjä et al. (2022) and spending all the time over land specifically over the forest. The p values indicate that these correlations are significant. Also the correlation between particles larger than 0.5 μm in diameter and the total concentration of fluorescent particles show enhanced positive correlations (0.3 and 0.27). These weak correlations indicate that aerosol particles larger than 0.5 μm that are biological may preferentially serve as INP. This is consistent with the heat test data reported by Schneider et al. (2021) for the same location where they observed a substantial decrease in the INP concentration after heating, indicating the presence of a population of protein based ice nucleating entities (Daily et al., 2022). This is also consistent with the size resolved INP measurements reported by Porter et al.



(2022) who demonstrated that below $-23\text{ }^{\circ}\text{C}$, the 2.5 to 10 μm size category was more important than smaller sized aerosol to the INP population. The correlation with aerosol concentrations between 3.5 nm and 50 nm is much weaker (0.2). There were aerosol nucleation events during the HyICE-2018 campaign (Brasseur et al., 2022) that created large concentrations of aerosol particles smaller than 50 nm, hence the lack of correlation with those aerosol particles indicates that they do not serve as INPs. The total aerosol concentration and the aerosol concentration of particles with diameters between 50 nm and 500 nm have values of 0.29 and 0.35, respectively, meaning that besides the bioaerosol particles from the coarse mode, there may also be INP in the population of aerosol particles smaller than 500 nm.

The correlations with meteorological variables are generally low (correlation coefficients of <0.17), with the exception of a moderate negative correlation with relative humidity (-0.38). This means that at low relative humidity, the INP concentration was generally greater and vice versa. This might be explained by the known mechanisms of bioaerosol release at low RH (Marshall, 1996; Tormo et al., 2001). Studies of the ice nucleating ability of lichens from Hyytiälä and elsewhere in the world show that several common lichen species harbour large quantities of very active ice nucleating entities (Moffett et al., 2015; Eufemio et al., 2023; Proske et al., 2024). It is also thought that bioaerosol released from lichens is enhanced at low RH (Armstrong, 1991; Tormo et al., 2001) and since lichens are one of the few biological entities not covered in snow, they should be considered a candidate source of bioaerosol in the boreal forest. The evidence from the correlation with both aerosol properties and relative humidity is consistent with a biological contribution of INP to the INP population active at temperatures between $-27\text{ }^{\circ}\text{C}$ and $-30\text{ }^{\circ}\text{C}$.

3.5 Response of the INP concentration to changing ambient conditions

In this section we present two independent case studies to examine how the measured INP concentration varied with a range of parameters. During the first case (18 h from March 25 06:00 to March 26 00:00) there was a synoptic air mass change associated with a weather front, whereas during the second case (22 h from May 02 00:00 to May 02 22:00) there was no major air mass change.

The first case (Figure 7) is characterized by a change in the overall synoptic situation induced by a cold front passing over Hyytiälä at around 14 local time. Cold front passages are characterized by a drop in temperature, an increase in pressure (Figure 7c), a prompt change in wind direction (Figure 7d) and precipitation typically beginning after the change in wind direction (Figure 7e). In the hours prior to the passage of the front, the INP concentration increased by approximately two orders of magnitude from 5 L^{-1} to almost 400 L^{-1} , falling back to lower values ($\approx 100\text{ L}^{-1}$) after the front passed (Figure 7a). The INP concentration continued to decrease steadily through the afternoon and evening, perhaps due to scavenging by the snow that fell during this period. A similar behavior of the INP concentration was observed in the 30 min time resolved PINC data (Paramonov et al., 2020). The total particle concentration peaks at the same time as the INP concentration (Figure 7b), while the concentration of particles larger than $0.5\text{ }\mu\text{m}$ is more constant with higher values in the morning hours. The fact that the increase in INP concentration mirrors the peak in total aerosol concentration suggests that the additional INP are less than $0.5\text{ }\mu\text{m}$. The total concentration of fluorescent particles measured with WIBS shows a small increase in concentration between 15 and 18 local time and with that has a profile independent of the INPs, indicating that the additional biogenic aerosol detected

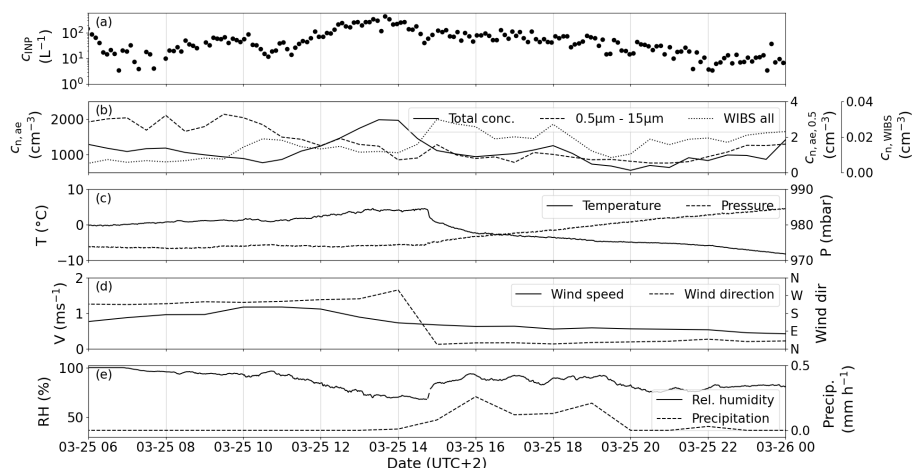


Figure 7. March 25 case study, where a cold front passed over Hyytiälä in the early afternoon. (a) Measured PINE INP concentration. (b) The total aerosol number concentration (solid line, left axis) and the number concentration of aerosol particles larger than $0.5 \mu\text{m}$ in diameter (dashed line, right axis) and the total fluorescent particles measured with WIFS (dotted line, secondary right axis). The ambient air temperature T (solid line, left axis) and pressure p (dashed line, right axis) are plotted in (c). (d) Wind speed v (solid line, left axis) and the wind direction (dashed line, right axis). (e) Relative humidity RH (solid line, left axis) and the accumulated snow fall (dashed line, right axis).

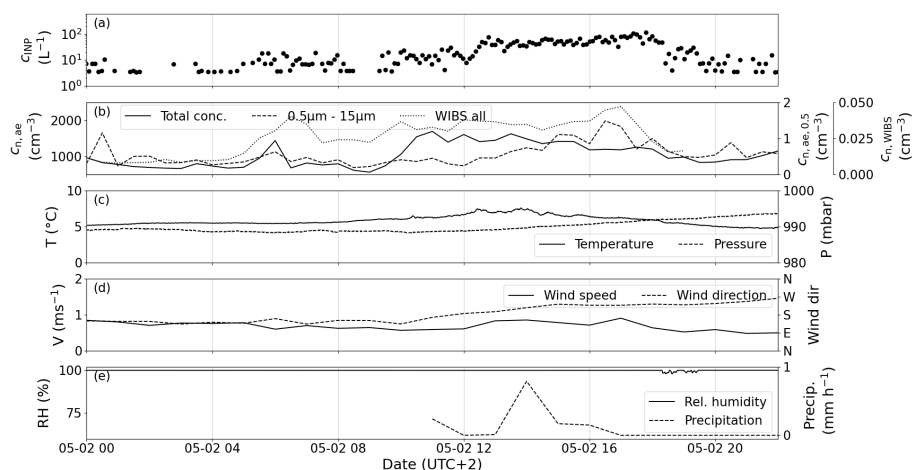


Figure 8. May 2 case study. (a) Measured PINE INP concentration. (b) The total aerosol number concentration (solid line, left axis) and the number concentration of aerosol particles larger than $0.5 \mu\text{m}$ in diameter (dashed line, right axis) and the total fluorescent particles measured with WIFS (dotted line, secondary right axis). The ambient air temperature T (solid line, left axis) and pressure p (dashed line, right axis) are plotted in (c). (d) Wind speed v (solid line, left axis) and the wind direction (dashed line, right axis). (e) Relative humidity RH (solid line, left axis) and the accumulated snow fall (dashed line, right axis).

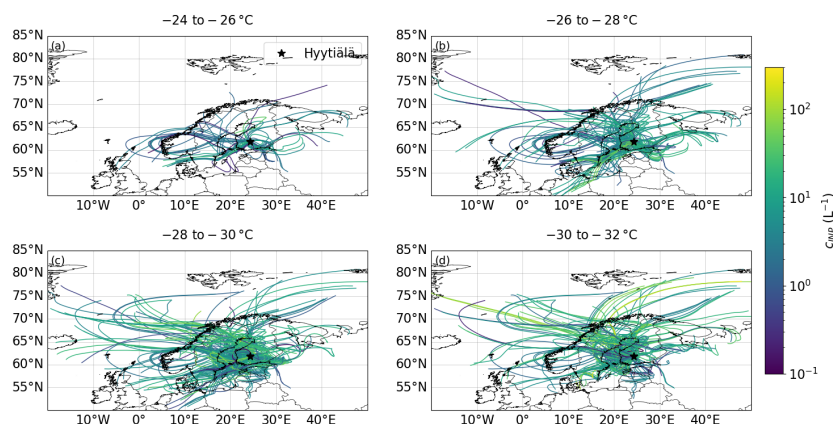


Figure 9. HYSPLIT 72 h backward trajectories calculated every 3 h. The colors represent the measured PINE INP concentration averaged over 3 h and then linked to the start time of the trajectory. The measurements are divided into four temperature ranges (a) to (d) covering 2 °C each.

by the WIBS does not contribute to the INP concentration in this occasion. Inspection of Figure 7e reveals that the relative humidity decreased from approx. 90 % to approx. 70 % during the period of elevated INP concentrations. The increase in the INP concentration is perhaps related to a release of aerosol particles at decreased relative humidity, perhaps consistent with the release of sub 500 nm aerosol from lichen sources, where it was observed that here was a significant negative correlation between relative humidity and INP.

In the second case, on May 2, the INP concentration varied by approximately two orders of magnitude between 5 L^{-1} and 100 L^{-1} (Figure 8a), without any abrupt changes in ambient air temperature, pressure or wind direction that might be associated with a front (Figure 8c and 8d). The number concentration of particles larger than $0.5 \mu\text{m}$ in diameter (Figure 8b) increases from approximately 0.5 cm^{-3} in the night and morning hours to 1.5 cm^{-3} in the afternoon at 17 local time. In comparison to the first case, the WIBS particle concentration increases during the day, mirroring the INP concentration. Thus changes in the measured INP concentration may be explained by the enhanced release of biogenic aerosol. However, the relative humidity was nearly 100 % for most of the day.

The case studies presenting two selected time periods of 18 h and 22 h show a response of the INP concentration to different variables: case one more to meteorology and case two more to the ambient aerosol. This points out that on short time scales the INP concentrations can be driven by different factors, which leads to the correlation coefficients associated with the full time period being rather low.



3.6 Backward trajectory analysis

Backward trajectory analysis has been used in the past to identify scenarios that lead to enhanced INP concentrations or specific
345 locations or processes that serve as sources of INP. For example, in a dataset of INP concentrations at the North Pole, Porter
et al. (2022) used backward trajectory analysis to show that the periods of high INP concentrations corresponded to transport
of air from the Russian coastline, whereas the lowest INP concentrations corresponded to air that had spent the preceding week
circulating around the pack ice. For the PINE dataset presented here, we calculated backward trajectories using the HYSPLIT
(Hybrid Single-Particle Lagrangian Integrated Trajectory) model (Stein et al., 2015), where one 72 h backward trajectory was
350 calculated every 3 h. Each of the trajectories is color coded with the INP concentration that was measured at the start time of the
trajectory. In order to extinguish a temperature dependency, the trajectories are divided into four temperature regimes, namely -
24 to -26 °C, -26 to -28 °C, -28 to -30 °C and -30 to -32 °C (figure 9). None of the four temperature bins shows a distinct pattern,
i.e. air containing higher INP concentrations does not clearly differ from air masses containing lower INP concentrations. The
seemingly random distribution is consistent with the idea that sources of bioaerosol local to the measurement site control the
355 INP population.

4 Conclusions

PINE is an instrument to measure ice-nucleating particles in an automated manner with a high time resolution and can be
applied for both field and laboratory studies. In this paper, we used PINE to quantify the INP population in a Finnish boreal
forest during spring alongside an array of other INP and aerosol measurements. This is the first field deployment of PINE and
360 we pay special attention to how PINE data can be analyzed and interpreted. This includes different time averaging methods,
allowing us to quantify low INP concentrations and average over many expansions with confidence. The results show that the
INP concentrations reported by PINE are consistent with other INP measurements. Overall these measurements show that the
INP concentration in this location is up to three orders of magnitude greater than in remote ocean environments, but is generally
lower or overlapping with other terrestrial environments, like the UK and the tropical Eastern Atlantic.

365 We use the high-time resolution INP data and aerosol measurements to challenge a number of parameterizations from the
literature. We found that the Tobo 2013 (1) parameterization, based on measurements in a ponderosa pine forest in Colorado
at 2370 m above sea level in summer, using the aerosol number concentration of particles larger than 0.5 μm in diameter
as a predictive parameter is the most suitable predictor for our INP measurements. The fact that a parameterization based on
measurements in a conifer forest in Colorado can predict the mean INP concentrations in a boreal forest in Finland implies some
370 commonality between the two environments. Indeed, Tobo et al. (2013) concluded that biological particles contributed to the
INP population in Colorado and we note that there is a moderate correlation between the fluorescent bioaerosol population and
the INP concentration during HyICE-2018. The INP population in Colorado and Finland were also similar in that the DeMott
2010 parameterization produced a too shallow temperature dependence when compared to the respective datasets. However, a
second parameterization proposed by Tobo et al. (2013), linking INP to fluorescent bioaerosol concentration, underpredicted



375 our mean INP concentrations by about a factor of two. This indicates that the atmospheres of both environments have biological
INPs that may have some commonality, but they are not identical.

Further evidence for the predominance of biological INP during HyICE-2018 across the full mixed-phase temperature regime
comes from the study of Schneider et al. (2021) who found that INP at all temperatures (down to -25°C in their study) were
removed with heat treatments. This sensitivity to heat indicates the presence of protein based INPs consistent with those
380 found in lichen, bacteria and fungus (Daily et al., 2022). The evidence presented here suggests that INPs in this boreal forest
that are active below -24°C can be also biological. In a previously published study from HyICE-2018 (Paramonov et al.,
2020), using data from a thermal gradient diffusion chamber, it is suggested that INP were from distant sources. However, the
positive correlation with time-over-land suggests that the boreal forest serves as a source of INP. Given that many surfaces were
covered in snow during the first half of the campaign, including the tree canopy and the ground, several potential INP sources
385 are not available. The snow melt did not bring any significant change in the INP concentration in the PINE dataset, suggesting
that local INP sources are available independent of the snow. One potential reservoir of INP that was exposed to air during
HyICE-2018, despite the snow cover, are tree dwelling lichens (Proske et al., 2024). It has been argued that lichens might
produce atmospheric ice nucleating bioaerosol (Moffett et al., 2015), and it is known that the effect of humidity on bioaerosol
production is complex with high humidity leading to production of structures on lichen that can become aerosolized later if
390 the humidity decreases (Marshall, 1996; Armstrong, 1991; Proske et al., 2024). More work is clearly needed to understand the
potential role lichen and other bioaerosol types may play as a source of INPs in boreal forests, and perhaps wider afield.

Data availability. The INP data of PINE and NIPI are available at <https://doi.org/10.5281/zenodo.10469663> (Brasseur et al., 2022). The
INP data of INSEKT, the WIBS and APS and DMPS data are also presented in Schneider et al. (2021) and are available under <https://doi.org/10.5445/IR/1000120666>. The aerosol, trace gas and meteorological data are available at the SmartSMEAR data repository (<https://avaa.tdata.fi/web/smart>; Junninen et al. (2009)).
395

Author contributions. FV, MPA and BJM wrote the paper. FV, MPA, LL, KH, JS, TS, BB and NSU conducted the measurements during
the campaign. FV, JN, NB and RF supported the data treatment of the PINE measurements. MPA, PF, ADH, UP and GCEP contributed the
results of the μl -NIPI data. PH and JK performed the WIBS measurements and analyzed the data. FV, MPA, LL, JS, ZB, EST, JD, TP, OM
and BJM contributed to the discussion and interpretation of the results. OM, MK, TP and JD planned the HyICE-2018 campaign.

400 *Competing interests.* At least one of the (co-)authors is a member of the editorial board of Atmospheric Chemistry and Physics.

Acknowledgements. The authors gratefully acknowledge the technical staff of the Hyytiälä Forestry Field Station for their help and support
during the HyICE-2018 campaign.



Financial support. This research has been supported by the Horizon 2020 (grant nos. ACTRIS-2 654109, ACTRIS PPP 739530, ACTRIS IMP 871115, 328616, ACTRIS-HY, ERA-PLANET 689443 and ACTRIS-CF 329274), the Helmholtz Association (grant no. 120101), the
405 KIT Technology Transfer (grant no. N059), the Academy of Finland (grant nos. 307331, 307537 and 286558), the European Research Council (grant no. MarineIce 648661), the Engineering and Physical Science Research Council (EP/S023593/1), the Natural Environment Research Council (NE/M010473/1, NE/L002574/1), the University of Leeds International Strategy Fund, the Maj ja Tor Nesslingin Säätiö (grant no. 201900390), the Swedish Research Council (grant nos. 2013-05153 and 2017-00564) and the Alexander von Humboldt-Stiftung (grant no. 1188375). EST is supported by the Swedish Research Council VR(2020-03497).



410 References

- Armstrong, R.: The influence of climate on the dispersal of lichen soredia, *Environmental and Experimental Botany*, 31, 239–245, [https://doi.org/https://doi.org/10.1016/0098-8472\(91\)90076-Z](https://doi.org/https://doi.org/10.1016/0098-8472(91)90076-Z), 1991.
- Atkinson, J. D., Murray, B. J., Woodhouse, M. T., Whale, T. F., Baustian, K. J., Carslaw, K. S., Dobbie, S., O’Sullivan, D., and Malkin, T. L.: The importance of feldspar for ice nucleation by mineral dust in mixed-phase clouds, *Nature*, 498, 355–358, <https://doi.org/10.1038/nature12278>, 2013.
- 415 Barr, S. L., Wyld, B., McQuaid, J. B., Neely III, R. R., and Murray, B. J.: Southern Alaska as a source of atmospheric mineral dust and ice-nucleating particles, *Science Advances*, 9, eadg3708, <https://doi.org/10.1126/sciadv.adg3708>, 2023.
- Boucher, O., Randall, D., Artaxo, P., Bretherton, C., Feingold, G., Forster, P., Kerminen, V.-M., Kondo, Y., Liao, H., Lohmann, U., Rasch, P., Satheesh, S. K., Sherwood, S., Stevens, B., and Zhang, X. Y.: Clouds and Aerosols, in: *Climate Change 2013: The Physical Science Basis. Contribution of Working Group I to the Fifth Assessment Report of the Intergovernmental Panel on Climate Change*, pp. 571–658, Cambridge University Press, Cambridge, United Kingdom and New York, NY, USA, 10.1017/CBO9781107415324.016, 2013.
- 420 Brasseur, Z., Castarède, D., Thomson, E. S., Adams, M. P., Drossaert van Dusseldorp, S., Heikkilä, P., Korhonen, K., Lampilahti, J., Paramonov, M., Schneider, J., Vogel, F., Wu, Y., Abbatt, J. P. D., Atanasova, N. S., Bamford, D. H., Bertozzi, B., Boyer, M., Brus, D., Daily, M. I., Fösig, R., Gute, E., Harrison, A. D., Hietala, P., Höhler, K., Kanji, Z. A., Keskinen, J., Lacher, L., Lampimäki, M., Levula, J., Manninen, A., Nadolny, J., Peltola, M., Porter, G. C. E., Poutanen, P., Proske, U., Schorr, T., Silas Umo, N., Stenszky, J., Virtanen, A., Moisseev, D., Kulmala, M., Murray, B. J., Petäjä, T., Möhler, O., and Duplissy, J.: Measurement report: Introduction to the HyICE-2018 campaign for measurements of ice-nucleating particles and instrument inter-comparison in the Hyytiälä boreal forest, *Atmospheric Chemistry and Physics*, 22, 5117–5145, <https://doi.org/10.5194/acp-22-5117-2022>, 2022.
- 425 Castarède, D., Brasseur, Z., Wu, Y., Kanji, Z. A., Hartmann, M., Ahonen, L., Bilde, M., Kulmala, M., Petäjä, T., Pettersson, J. B. C., Sierau, B., Stetzer, O., Stratmann, F., Svenningsson, B., Swietlicki, E., Thu Nguyen, Q., Duplissy, J., and Thomson, E. S.: Development and characterization of the Portable Ice Nucleation Chamber 2 (PINCii), *Atmospheric Measurement Techniques*, 16, 3881–3899, <https://doi.org/10.5194/amt-16-3881-2023>, 2023.
- 430 Ceppi, P., Briant, F., Zelinka, M. D., and Hartmann, D. L.: Cloud feedback mechanisms and their representation in global climate models, *WIREs Climate Change*, 8, e465, <https://doi.org/https://doi.org/10.1002/wcc.465>, 2017.
- 435 Choi, Y.-S., Lindzen, R. S., Ho, C.-H., and Kim, J.: Space observations of cold-cloud phase change, *Proceedings of the National Academy of Sciences*, 107, 11 211–11 216, <https://doi.org/10.1073/pnas.1006241107>, 2010.
- Chou, C., Stetzer, O., Weingartner, E., Jurányi, Z., Kanji, Z. A., and Lohmann, U.: Ice nuclei properties within a Saharan dust event at the Jungfraujoch in the Swiss Alps, *Atmospheric Chemistry and Physics*, 11, 4725–4738, <https://doi.org/10.5194/acp-11-4725-2011>, 2011.
- Cornwell, G. C., McCluskey, C. S., Hill, T. C., Levin, E. T., Rothfuss, N. E., Tai, S.-L., Petters, M. D., DeMott, P. J., Kreidenweis, S., Prather, K. A., et al.: Bioaerosols are the dominant source of warm-temperature immersion-mode INPs and drive uncertainties in INP predictability, *Science Advances*, 9, eadg3715, 2023.
- 440 Daily, M. I., Tarn, M. D., Whale, T. F., and Murray, B. J.: An evaluation of the heat test for the ice-nucleating ability of minerals and biological material, *Atmospheric Measurement Techniques*, 15, 2635–2665, <https://doi.org/10.5194/amt-15-2635-2022>, 2022.
- 445 DeMott, P. J., Prenni, A. J., Liu, X., Kreidenweis, S. M., Petters, M. D., Twohy, C. H., Richardson, M. S., Eidhammer, T., and Rogers, D. C.: Predicting global atmospheric ice nuclei distributions and their impacts on climate, *Proceedings of the National*



- Academy of Sciences, 107, 11 217–11 222, <https://doi.org/10.1073/pnas.0910818107>, publisher: National Academy of Sciences _eprint: <https://www.pnas.org/content/107/25/11217.full.pdf>, 2010.
- DeMott, P. J., Hill, T. C. J., McCluskey, C. S., Prather, K. A., Collins, D. B., Sullivan, R. C., Ruppel, M. J., Mason, R. H., Irish, V. E., Lee, T., Hwang, C. Y., Rhee, T. S., Snider, J. R., McMeeking, G. R., Dhaniyala, S., Lewis, E. R., Wentzell, J. J. B., Abbatt, J., Lee, C., Sultana, C. M., Ault, A. P., Axson, J. L., Diaz Martinez, M., Venero, I., Santos-Figueroa, G., Stokes, M. D., Deane, G. B., Mayol-Bracero, O. L., Grassian, V. H., Bertram, T. H., Bertram, A. K., Moffett, B. F., and Franc, G. D.: Sea spray aerosol as a unique source of ice nucleating particles, *Proceedings of the National Academy of Sciences*, 113, 5797–5803, <https://doi.org/10.1073/pnas.1514034112>, 2016.
- Eufemio, R. J., de Almeida Ribeiro, I., Sformo, T. L., Laursen, G. A., Molinero, V., Fröhlich-Nowoisky, J., Bonn, M., and Meister, K.: Lichen species across Alaska produce highly active and stable ice nucleators, *Biogeosciences*, 20, 2805–2812, <https://doi.org/10.5194/bg-20-2805-2023>, 2023.
- Fahy, W. D., Maters, E. C., Miranda, R. G., Adams, M. P., Jahn, L. G., Sullivan, R. C., and Murray, B. J.: Volcanic ash ice nucleation activity is variably reduced by aging in water and sulfuric acid: the effects of leaching, dissolution, and precipitation, *Environmental Science: Atmospheres*, 2, 85–99, 2022.
- Grawe, S., Augustin-Bauditz, S., Hartmann, S., Hellner, L., Pettersson, J. B., Prager, A., Stratmann, F., and Wex, H.: The immersion freezing behavior of ash particles from wood and brown coal burning, *Atmospheric Chemistry and Physics*, 16, 13 911–13 928, 2016.
- Hari, P., Nikinmaa, E., Pohja, T., Siivola, E., Bäck, J., Vesala, T., and Kulmala, M.: Station for Measuring Ecosystem-Atmosphere Relations: SMEAR, pp. 471–487, Springer Netherlands, Dordrecht, https://doi.org/10.1007/978-94-007-5603-8_9, 2013.
- Hawker, R. E., Miltenberger, A. K., Johnson, J. S., Wilkinson, J. M., Hill, A. A., Shipway, B. J., Field, P. R., Murray, B. J., and Carslaw, K. S.: Model emulation to understand the joint effects of ice-nucleating particles and secondary ice production on deep convective anvil cirrus, *Atmospheric Chemistry and Physics*, 21, 17 315–17 343, <https://doi.org/10.5194/acp-21-17315-2021>, 2021a.
- Hawker, R. E., Miltenberger, A. K., Wilkinson, J. M., Hill, A. A., Shipway, B. J., Cui, Z., Cotton, R. J., Carslaw, K. S., Field, P. R., and Murray, B. J.: The temperature dependence of ice-nucleating particle concentrations affects the radiative properties of tropical convective cloud systems, *Atmospheric Chemistry and Physics*, 21, 5439–5461, <https://doi.org/10.5194/acp-21-5439-2021>, 2021b.
- Herbert, R. J., Murray, B. J., Dobbie, S. J., and Koop, T.: Sensitivity of liquid clouds to homogenous freezing parameterizations, *Geophysical Research Letters*, 42, 1599–1605, <https://doi.org/10.1002/2014GL062729>, 2015.
- Hill, T. C. J., DeMott, P. J., Tobo, Y., Fröhlich-Nowoisky, J., Moffett, B. F., Franc, G. D., and Kreidenweis, S. M.: Sources of organic ice nucleating particles in soils, *Atmospheric Chemistry and Physics*, 16, 7195–7211, <https://doi.org/10.5194/acp-16-7195-2016>, 2016.
- Hiranuma, N., Auvermann, B. W., Belosi, F., Bush, J., Cory, K. M., Georgakopoulos, D. G., Höhler, K., Hou, Y., Lacher, L., Saathoff, H., Santachiara, G., Shen, X., Steinke, I., Ullrich, R., Umo, N. S., Vepuri, H. S. K., Vogel, F., and Möhler, O.: Laboratory and field studies of ice-nucleating particles from open-lot livestock facilities in Texas, *Atmospheric Chemistry and Physics*, 21, 14 215–14 234, <https://doi.org/10.5194/acp-21-14215-2021>, 2021.
- Hoose, C. and Möhler, O.: Heterogeneous ice nucleation on atmospheric aerosols: a review of results from laboratory experiments, *Atmospheric Chemistry and Physics*, 12, 9817–9854, <https://doi.org/10.5194/acp-12-9817-2012>, 2012.
- Hoose, C., Kristjánsson, J. E., and Burrows, S. M.: How important is biological ice nucleation in clouds on a global scale?, *Environmental Research Letters*, 5, 024 009, <https://doi.org/10.1088/1748-9326/5/2/024009>, 2010.
- Irish, V. E., Elizondo, P., Chen, J., Chou, C., Charette, J., Lizotte, M., Ladino, L. A., Wilson, T. W., Gosselin, M., Murray, B. J., Polishchuk, E., Abbatt, J. P. D., Miller, L. A., and Bertram, A. K.: Ice-nucleating particles in Canadian Arctic sea-surface microlayer and bulk seawater, *Atmospheric Chemistry and Physics*, 17, 10 583–10 595, <https://doi.org/10.5194/acp-17-10583-2017>, 2017.



- Irish, V. E., Hanna, S. J., Xi, Y., Boyer, M., Polishchuk, E., Ahmed, M., Chen, J., Abbatt, J. P. D., Gosselin, M., Chang, R., Miller, L. A., and
485 Bertram, A. K.: Revisiting properties and concentrations of ice-nucleating particles in the sea surface microlayer and bulk seawater in the
Canadian Arctic during summer, *Atmospheric Chemistry and Physics*, 19, 7775–7787, <https://doi.org/10.5194/acp-19-7775-2019>, 2019.
- Junninen, H., Lauri, A., Keronen, P., Aalto, P., Hiltunen, V., Hari, P., and Kulmala, M.: Smart-SMEAR: On-line data exploration and visual-
ization tool for SMEAR stations, *Boreal Environment Research*, 14, 447–457, 2009.
- Kanitz, T., Seifert, P., Ansmann, A., Engelmann, R., Althausen, D., Casiccia, C., and Rohwer, E. G.: Contrasting the impact of aerosols at
490 northern and southern midlatitudes on heterogeneous ice formation: AEROSOL EFFECT ON ICE FORMATION, *Geophysical Research
Letters*, 38, n/a–n/a, <https://doi.org/10.1029/2011GL048532>, 2011.
- Kanji, Z. A., Welti, A., Chou, C., Stetzer, O., and Lohmann, U.: Laboratory studies of immersion and deposition mode ice nucleation of
ozone aged mineral dust particles, *Atmospheric Chemistry and Physics*, 13, 9097–9118, <https://doi.org/10.5194/acp-13-9097-2013>, 2013.
- Kanji, Z. A., Ladino, L. A., Wex, H., Boose, Y., Burkert-Kohn, M., Cziczko, D. J., and Krämer, M.: Overview of Ice Nucleating Particles,
495 *Meteorological Monographs*, 58, 1.1–1.33, <https://doi.org/10.1175/AMSMONOGRAPHS-D-16-0006.1>, 2017.
- Kulmala, M., Hameri, K., Aalto, P. P., Makela, J. M., Pirjola, L., Nilsson, E. D., Buzorius, G., Rannik, U., Maso, M. D., Seidl, W., Hoffman,
T., Janson, R., Hansson, H.-C., Viisanen, Y., Laaksonen, A., and O’Dowd, C. D.: Overview of the international project on biogenic aerosol
formation in the boreal forest (BIOFOR), *Tellus B*, 53, 324–343, <https://doi.org/10.1034/j.1600-0889.2001.530402.x>, 2001.
- Lacher, L., Adams, M. P., Barry, K., Bertozzi, B., Bingemer, H., Boffo, C., Bras, Y., Büttner, N., Castarede, D., Cziczko, D. J., DeMott,
500 P. J., Fösig, R., Goodell, M., Höhler, K., Hill, T. C. J., Jentsch, C., Ladino, L. A., Levin, E. J. T., Mertes, S., Möhler, O., Moore, K. A.,
Murray, B. J., Nadolny, J., Pfeuffer, T., Picard, D., Ramírez-Romero, C., Ribeiro, M., Richter, S., Schrod, J., Sellegri, K., Stratmann,
F., Swanson, B. E., Thomson, E. S., Wex, H., Wolf, M. J., and Freney, E.: The Puy de Dôme ICE Nucleation Intercomparison Cam-
paign (PICNIC): comparison between online and offline methods in ambient air, *Atmospheric Chemistry and Physics*, 24, 2651–2678,
<https://doi.org/10.5194/acp-24-2651-2024>, 2024.
- 505 Maki, T., Hosaka, K., Lee, K. C., Kawabata, Y., Kajino, M., Uto, M., Kita, K., and Igarashi, Y.: Vertical distribution of airborne mi-
croorganisms over forest environments: A potential source of ice-nucleating bioaerosols, *Atmospheric Environment*, 302, 119 726,
<https://doi.org/10.1016/j.atmosenv.2023.119726>, 2023.
- Mangan, T. P., Atkinson, J. D., Neuberg, J. W., O’Sullivan, D., Wilson, T. W., Whale, T. F., Neve, L., Umo, N. S., Malkin, T. L., and
Murray, B. J.: Heterogeneous Ice Nucleation by Soufriere Hills Volcanic Ash Immersed in Water Droplets, *PLOS ONE*, 12, e0169 720,
510 <https://doi.org/10.1371/journal.pone.0169720>, 2017.
- Marshall, W. A.: Aerial dispersal of lichen soredia in the maritime Antarctic, *New Phytologist*, 134, 523–530,
<https://doi.org/https://doi.org/10.1111/j.1469-8137.1996.tb04370.x>, 1996.
- Matus, A. V. and L’Ecuyer, T. S.: The role of cloud phase in Earth’s radiation budget: CLOUD PHASE IN EARTH’S RADIATION BUDGET,
Journal of Geophysical Research: Atmospheres, 122, 2559–2578, <https://doi.org/10.1002/2016JD025951>, 2017.
- 515 McCluskey, C. S., Hill, T. C. J., Humphries, R. S., Rauker, A. M., Moreau, S., Strutton, P. G., Chambers, S. D., Williams, A. G., McRobert,
I., Ward, J., Keywood, M. D., Harnwell, J., Ponsonby, W., Loh, Z. M., Krummel, P. B., Protat, A., Kreidenweis, S. M., and De-
Mott, P. J.: Observations of Ice Nucleating Particles Over Southern Ocean Waters, *Geophysical Research Letters*, 45, 11,989–11,997,
<https://doi.org/https://doi.org/10.1029/2018GL079981>, 2018.
- Moffett, B. F., Getti, G., Henderson-Begg, S. K., and Hill, T. C. J.: Ubiquity of ice nucleation in lichen — possible atmospheric implications,
520 *Lindbergia*, 38, 39 – 43, <https://doi.org/10.25227/linbg.01070>, 2015.



- Murray, B. J., O'Sullivan, D., Atkinson, J. D., and Webb, M. E.: Ice nucleation by particles immersed in supercooled cloud droplets, *Chemical Society Reviews*, 41, 6519, <https://doi.org/10.1039/c2cs35200a>, 2012.
- Murray, B. J., Carslaw, K. S., and Field, P. R.: Opinion: Cloud-phase climate feedback and the importance of ice-nucleating particles, *Atmospheric Chemistry and Physics*, 21, 665–679, <https://doi.org/10.5194/acp-21-665-2021>, 2021.
- 525 Möhler, O., Adams, M., Lacher, L., Vogel, F., Nadolny, J., Ullrich, R., Boffo, C., Pfeuffer, T., Hobl, A., Weiß, M., Vepuri, H. S. K., Hiranuma, N., and Murray, B. J.: The Portable Ice Nucleation Experiment (PINE): a new online instrument for laboratory studies and automated long-term field observations of ice-nucleating particles, *Atmospheric Measurement Techniques*, 14, 1143–1166, <https://doi.org/10.5194/amt-14-1143-2021>, 2021.
- Neefjes, I., Laapas, M., Liu, Y., Médus, E., Miettunen, E., Ahonen, L., Quéléver, L., Aalto, J., Bäck, J., Kerminen, V., et al.: 25 years of atmospheric and ecosystem measurements in a boreal forest—Seasonal variation and responses to warm and dry years, *Boreal Environment Research*, 27, 1, 2022.
- 530 Niemand, M., Möhler, O., Vogel, B., Vogel, H., Hoose, C., Connolly, P., Klein, H., Bingemer, H., DeMott, P., Skrotzki, J., and Leisner, T.: A Particle-Surface-Area-Based Parameterization of Immersion Freezing on Desert Dust Particles, *Journal of the Atmospheric Sciences*, 69, 3077–3092, <https://doi.org/10.1175/JAS-D-11-0249.1>, 2012.
- 535 O'Sullivan, D., Murray, B. J., Malkin, T. L., Whale, T. F., Umo, N. S., Atkinson, J. D., Price, H. C., Baustian, K. J., Browse, J., and Webb, M. E.: Ice nucleation by fertile soil dusts: relative importance of mineral and biogenic components, *Atmospheric Chemistry and Physics*, 14, 1853–1867, <https://doi.org/10.5194/acp-14-1853-2014>, 2014.
- O'Sullivan, D., Adams, M. P., Tarn, M. D., Harrison, A. D., Vergara-Temprado, J., Porter, G. C. E., Holden, M. A., Sanchez-Marroquin, A., Carotenuto, F., Whale, T. F., McQuaid, J. B., Walshaw, R., Hedges, D. H. P., Burke, I. T., Cui, Z., and Murray, B. J.: Contributions of biogenic material to the atmospheric ice-nucleating particle population in North Western Europe, *Scientific Reports*, 8, 13 821, <https://doi.org/10.1038/s41598-018-31981-7>, 2018.
- 540 Paramonov, M., Drossaert van Dusseldorp, S., Gute, E., Abbatt, J. P. D., Heikkilä, P., Keskinen, J., Chen, X., Luoma, K., Heikkinen, L., Hao, L., Petäjä, T., and Kanji, Z. A.: Condensation/immersion mode ice-nucleating particles in a boreal environment, *Atmospheric Chemistry and Physics*, 20, 6687–6706, <https://doi.org/10.5194/acp-20-6687-2020>, 2020.
- 545 Petäjä, T., Tabakova, K., Manninen, A., Ezhova, E., O'Connor, E., Moisseev, D., Sinclair, V. A., Backman, J., Levula, J., Luoma, K., et al.: Influence of biogenic emissions from boreal forests on aerosol–cloud interactions, *Nature Geoscience*, 15, 42–47, 2022.
- Petters, M. D. and Wright, T. P.: Revisiting ice nucleation from precipitation samples: ICE NUCLEATION FROM PRECIPITATION, *Geophysical Research Letters*, 42, 8758–8766, <https://doi.org/10.1002/2015GL065733>, 2015.
- Ponsonby, J., King, L., Murray, B. J., and Stettler, M. E. J.: Jet aircraft lubrication oil droplets as contrail ice-forming particles, *Atmospheric Chemistry and Physics*, 24, 2045–2058, <https://doi.org/10.5194/acp-24-2045-2024>, 2024.
- 550 Porter, G. C. E., Adams, M. P., Brooks, I. M., Ickes, L., Karlsson, L., Leck, C., Salter, M. E., Schmale, J., Siegel, K., Sikora, S. N. F., Tarn, M. D., Vüllers, J., Wernli, H., Zieger, P., Zinke, J., and Murray, B. J.: Highly Active Ice-Nucleating Particles at the Summer North Pole, *Journal of Geophysical Research: Atmospheres*, 127, e2021JD036 059, <https://doi.org/10.1029/2021JD036059>, 2022.
- Price, H. C., Baustian, K. J., McQuaid, J. B., Blyth, A., Bower, K. N., Choularton, T., Cotton, R. J., Cui, Z., Field, P. R., Gallagher, M., Hawker, R., Merrington, A., Miltenberger, A., Neely III, R. R., Parker, S. T., Rosenberg, P. D., Taylor, J. W., Trembath, J., Vergara-Temprado, J., Whale, T. F., Wilson, T. W., Young, G., and Murray, B. J.: Atmospheric Ice-Nucleating Particles in the Dusty Tropical Atlantic, *Journal of Geophysical Research: Atmospheres*, 123, 2175–2193, <https://doi.org/10.1002/2017JD027560>, 2018.



- Proske, U., Adams, M. P., Porter, G. C. E., Holden, M., Bäck, J., and Murray, B. J.: Measurement report: The ice-nucleating activity of lichen sampled in a northern European boreal forest, *EGUsphere*, 2024, 1–22, <https://doi.org/10.5194/egusphere-2023-2780>, 2024.
- 560 Pruppacher, H. and Klett, J.: *Microphysics of Clouds and Precipitation*, Atmospheric and Oceanographic Sciences Library, Springer Netherlands, 2010.
- Radenz, M., Bühl, J., Seifert, P., Baars, H., Engelmann, R., Barja González, B., Mamouri, R.-E., Zamorano, F., and Ansmann, A.: Hemispheric contrasts in ice formation in stratiform mixed-phase clouds: disentangling the role of aerosol and dynamics with ground-based remote sensing, *Atmospheric Chemistry and Physics*, 21, 17 969–17 994, <https://doi.org/10.5194/acp-21-17969-2021>, 2021.
- 565 Sanchez-Marroquin, A., Arnalds, O., Baustian-Dorsi, K. J., Browse, J., Dagsson-Waldhauserova, P., Harrison, A. D., Maters, E. C., Pringle, K. J., Vergara-Temprado, J., Burke, I. T., McQuaid, J. B., Carslaw, K. S., and Murray, B. J.: Iceland is an episodic source of atmospheric ice-nucleating particles relevant for mixed-phase clouds, *Science Advances*, 6, eaba8137, <https://doi.org/10.1126/sciadv.aba8137>, 2020.
- Schill, G. P., DeMott, P. J., Emerson, E. W., Rauker, A. M. C., Kodros, J. K., Suski, K. J., Hill, T. C. J., Levin, E. J. T., Pierce, J. R., Farmer, D. K., and Kreidenweis, S. M.: The contribution of black carbon to global ice nucleating particle concentrations relevant to mixed-phase
- 570 clouds, *Proceedings of the National Academy of Sciences*, 117, 22 705–22 711, <https://doi.org/10.1073/pnas.2001674117>, 2020.
- Schneider, J., Höhler, K., Heikkilä, P., Keskinen, J., Bertozzi, B., Bogert, P., Schorr, T., Umo, N. S., Vogel, F., Brasseur, Z., Wu, Y., Hakala, S., Duplissy, J., Moisseev, D., Kulmala, M., Adams, M. P., Murray, B. J., Korhonen, K., Hao, L., Thomson, E. S., Castarède, D., Leisner, T., Petäjä, T., and Möhler, O.: The seasonal cycle of ice-nucleating particles linked to the abundance of biogenic aerosol in boreal forests, *Atmospheric Chemistry and Physics*, 21, 3899–3918, <https://doi.org/10.5194/acp-21-3899-2021>, 2021.
- 575 Schumacher, C. J., Pöhlker, C., Aalto, P., Hiltunen, V., Petäjä, T., Kulmala, M., Pöschl, U., and Huffman, J. A.: Seasonal cycles of fluorescent biological aerosol particles in boreal and semi-arid forests of Finland and Colorado, *Atmospheric Chemistry and Physics*, 13, 11 987–12 001, <https://doi.org/10.5194/acp-13-11987-2013>, 2013.
- Stein, A. F., Draxler, R. R., Rolph, G. D., Stunder, B. J. B., Cohen, M. D., and Ngan, F.: NOAA’s HYSPLIT Atmospheric Transport and Dispersion Modeling System, *Bulletin of the American Meteorological Society*, 96, 2059–2077, <https://doi.org/10.1175/BAMS-D-14-00110.1>, 2015.
- 580 Steinke, I., Funk, R., Busse, J., Iturri, A., Kirchen, S., Leue, M., Möhler, O., Schwartz, T., Schnaiter, M., Sierau, B., Toprak, E., Ullrich, R., Ulrich, A., Hoose, C., and Leisner, T.: Ice nucleation activity of agricultural soil dust aerosols from Mongolia, Argentina, and Germany: Ice Nucleation Activity of Soil Dust, *Journal of Geophysical Research: Atmospheres*, 121, 13,559–13,576, <https://doi.org/10.1002/2016JD025160>, 2016.
- 585 Storelvmo, T.: Aerosol Effects on Climate via Mixed-Phase and Ice Clouds, *Annual Review of Earth and Planetary Sciences*, 45, 199–222, <https://doi.org/10.1146/annurev-earth-060115-012240>, 2017.
- Takeishi, A. and Storelvmo, T.: A Study of Enhanced Heterogeneous Ice Nucleation in Simulated Deep Convective Clouds Observed During DC3, *Journal of Geophysical Research: Atmospheres*, 123, <https://doi.org/10.1029/2018JD028889>, 2018.
- Tobo, Y., Prenni, A. J., DeMott, P. J., Huffman, J. A., McCluskey, C. S., Tian, G., Pöhlker, C., Pöschl, U., and Kreidenweis, S. M.: Biological
- 590 aerosol particles as a key determinant of ice nuclei populations in a forest ecosystem: BIOLOGICAL ICE NUCLEI IN FOREST, *Journal of Geophysical Research: Atmospheres*, 118, 10,100–10,110, <https://doi.org/10.1002/jgrd.50801>, 2013.
- Tobo, Y., Adachi, K., DeMott, P. J., Hill, T. C., Hamilton, D. S., Mahowald, N. M., Nagatsuka, N., Ohata, S., Uetake, J., Kondo, Y., et al.: Glacially sourced dust as a potentially significant source of ice nucleating particles, *Nature Geoscience*, 12, 253–258, 2019.
- Tormo, R., Recio, D., Silva, I., and Muñoz, A.: A quantitative investigation of airborne algae and lichen soredia obtained from pollen traps
- 595 in south-west Spain, *European Journal of Phycology*, 36, 385–390, 2001.



- Umo, N. S., Murray, B. J., Baeza-Romero, M. T., Jones, J. M., Lea-Langton, A. R., Malkin, T. L., O'Sullivan, D., Neve, L., Plane, J. M. C., and Williams, A.: Ice nucleation by combustion ash particles at conditions relevant to mixed-phase clouds, *Atmospheric Chemistry and Physics*, 15, 5195–5210, <https://doi.org/10.5194/acp-15-5195-2015>, 2015.
- 600 Vali, G., DeMott, P., Möhler, O., and Whale, T.: A proposal for ice nucleation terminology, *Atmospheric Chemistry and Physics*, 15, 10263–10270, 2015.
- Vergara-Temprado, J., Murray, B. J., Wilson, T. W., O'Sullivan, D., Browse, J., Pringle, K. J., Ardon-Dryer, K., Bertram, A. K., Burrows, S. M., Ceburnis, D., DeMott, P. J., Mason, R. H., O'Dowd, C. D., Rinaldi, M., and Carslaw, K. S.: Contribution of feldspar and marine organic aerosols to global ice nucleating particle concentrations, *Atmospheric Chemistry and Physics*, 17, 3637–3658, <https://doi.org/10.5194/acp-17-3637-2017>, 2017.
- 605 Vergara-Temprado, J., Miltenberger, A. K., Furtado, K., Grosvenor, D. P., Shipway, B. J., Hill, A. A., Wilkinson, J. M., Field, P. R., Murray, B. J., and Carslaw, K. S.: Strong control of Southern Ocean cloud reflectivity by ice-nucleating particles, *Proceedings of the National Academy of Sciences*, 115, 2687–2692, <https://doi.org/10.1073/pnas.1721627115>, 2018.
- Villanueva, D., Senf, F., and Tegen, I.: Hemispheric and Seasonal Contrast in Cloud Thermodynamic Phase From A-Train Spaceborne Instruments, *Journal of Geophysical Research: Atmospheres*, 126, e2020JD034322, <https://doi.org/10.1029/2020JD034322>, 2021.
- 610 Welti, A., Müller, K., Fleming, Z. L., and Stratmann, F.: Concentration and variability of ice nuclei in the subtropical maritime boundary layer, *Atmospheric Chemistry and Physics*, 18, 5307–5320, <https://doi.org/10.5194/acp-18-5307-2018>, 2018.
- Westbrook, C. D. and Illingworth, A. J.: Evidence that ice forms primarily in supercooled liquid clouds at temperatures > -27°C, *Geophysical Research Letters*, 38, <https://doi.org/https://doi.org/10.1029/2011GL048021>, 2011.
- 615 Wex, H., Huang, L., Zhang, W., Hung, H., Traversi, R., Becagli, S., Sheesley, R. J., Moffett, C. E., Barrett, T. E., Bossi, R., Skov, H., Hünnerbein, A., Lubitz, J., Löffler, M., Linke, O., Hartmann, M., Herenz, P., and Stratmann, F.: Annual variability of ice-nucleating particle concentrations at different Arctic locations, *Atmospheric Chemistry and Physics*, 19, 5293–5311, <https://doi.org/10.5194/acp-19-5293-2019>, 2019.
- Wilbourn, E. K., Thornton, D. C., Ott, C., Graff, J., Quinn, P. K., Bates, T. S., Betha, R., Russell, L. M., Behrenfeld, M. J., and Brooks, S. D.: Ice Nucleation by Marine Aerosols Over the North Atlantic Ocean in Late Spring, *Journal of Geophysical Research: Atmospheres*, 125, e2019JD030913, <https://doi.org/https://doi.org/10.1029/2019JD030913>, e2019JD030913 2019JD030913, 2020.
- 620 Wilson, T. W., Ladino, L. A., Alpert, P. A., Breckels, M. N., Brooks, I. M., Browse, J., Burrows, S. M., Carslaw, K. S., Huffman, J. A., Judd, C., Kilthau, W. P., Mason, R. H., McFiggans, G., Miller, L. A., Nájera, J. J., Polishchuk, E., Rae, S., Schiller, C. L., Si, M., Temprado, J. V., Whale, T. F., Wong, J. P. S., Wurl, O., Yakobi-Hancock, J. D., Abbatt, J. P. D., Aller, J. Y., Bertram, A. K., Knopf, D. A., and Murray, B. J.: A marine biogenic source of atmospheric ice-nucleating particles, *Nature*, 525, 234–238, <https://doi.org/10.1038/nature14986>, 2015.